

DROP TEST ASSESSMENT OF A MEDIUM COMPLEXITY ASSEMBLY FOR HIGH RELIABILITY APPLICATIONS

P. Snugovsky, J. Bragg, Z. Bagheri, and M. Romansky
Celestica International Inc.
Toronto, ON, Canada

A. Ganster*, W. Russell#, J. P. Tucker**, C. A. Handwerker**, D. D. Fritz##
*Crane Division NSWC, #Raytheon, **Purdue University, ##SAIC
*Crane, IN, #Garland, TX, **West Lafayette, IN, ##Brookville, IN, USA

ABSTRACT

The mechanical behavior of printed circuit assemblies (PCA) at high strain rates is very important for the reliability of products used in harsh environments. The transition to Pb-free materials in the general electronics industry significantly impacts the mechanical reliability of solder joint interconnects, as widely recognized by the consumer electronics industry. Numerous mechanical behavior studies using a drop test have been reported on components with different Pb-free solders. This study is focused on leaded and leadless components in comparison with ball grid array components assembled with Pb-free solder on medium complexity boards. This study is part of a large scale NASA DoD project and utilized the same board design, assembly, and rework processes of that larger project. Components were attached to the boards using SnPb and Pb-free solder SAC305. The leaded and leadless components TSOP-50, TQFP-144, QFN-20, and CLCC-20 were then hand reworked using conventional SnPb solder to address the sustainment issue. The ball grid array components BGA and CSP underwent hot air rework also using conventional SnPb solder.

In the present work, a board-level drop shock test was performed on two sets of boards; each board had 63 components attached. The first set consisted of 9 boards and the testing was focused on leaded and leadless component behavior. The second set consisted of 20 boards and testing was focused on the BGA components. Each board was monitored for shock response and net electrical resistance for all components. In addition, three cards were monitored for board surface strain. The assemblies were fixtured to a drop table 3-up and subjected to either 340G or 500G shocks. The first set of 9 cards was subjected to 20 drops per board. The shock response, net resistance and strain were recorded in-situ during each drop. The vast majority of the electrical failures occurred on the PBGAs. Only three of the leaded and leadless components experienced electrical failure.

For the first set of 9 cards damage from the drop shock test was assessed by examining electrically failed and non-failed non-BGA parts by dye-and-pry and cross-section analyses followed by microstructural examination and defect

mapping. It was found that the predominant failure mechanism was board side pad cratering. The cracks propagated through the board material between the laminate and glass fiber under the pad. Electrical failure was only observed when the Cu trace was broken. Of the leaded components that were still electrically functional after drop testing, approximately one third were found to be mechanically damaged with pad cratering after dye and pry inspection. This hidden damage may be a reliability concern depending on the field use conditions. There was no correlation found between the number of reworks and the amount of electrical or mechanical failure since only three non-BGA components failed in the test. Most importantly, this sample set showed no difference in drop test performance between SnPb-reworked and non-reworked Pb-free solder joints for non-BGA components.

The second set of 20 boards was tested to evaluate BGA drop performance. The boards were subjected to 500G shocks, for total of 10 drops per board. Although the number of samples evaluated was low, due the large number of variables, drop testing of the PBGA parts showed the following trends: 1) BGAs with mixed SnPb/SAC 305 solder joints failed before pure SnPb BGAs, 2) When joints are mixed, mixed joints with SAC 305 in the ball and SnPb paste were more robust than those mixed with SnPb balls and SAC 305 paste, and 3) for both pure SnPb and pure Pb-free PBGAs, increasing the number of reworks reduced the resilience of the BGAs to drop testing.

INTRODUCTION

Impact due to drop/shock has recently become more important in the reliability of microelectronics. [1] There are a number of causes for this transition. First, greater functionality in circuit cards necessitates an increase in the density of components with a corresponding decrease in pitch size. These smaller solder joints experience higher strain rates under drop/shock, and are more prone to fracture. Second, concurrent to the decrease in pitch size, the consumer market has shifted from SnPb eutectic solder to Pb-free solders due to environmental legislation. Lead-free solders are less compliant than SnPb, and so they absorb a smaller fraction of the impact energy. Numerous mechanical behavior studies using drop tests have been

reported on ball grid array components with different Pb-free solder materials using drop test. In particular, Suh et. al. [1] found that SAC 105 exhibited a performance ten times better than SAC 405 in drop testing when designating 5% increase in resistance as the onset of failure. Since no apparent difference could be observed in the intermetallic layer or interfacial morphology, the authors proposed that the bulk solder behavior affected the fracture behavior of the solder joints by applying a concept called extrinsic toughening. SAC 105 is more compliant and deformable than SAC 405, so less energy is available to propagate a crack in SAC105 joints.

While the effects of Pb-free solder alloy on drop/shock performance have been studied, much less is known about the effect of reworked joints. In harsh environment applications such as military or aerospace, reliability is critical, and drop impact becomes a more significant concern. This paper reports on the findings of a joint study between Celestica Inc., Crane Division NSWC, Raytheon, Purdue University, and SAIC on how the drop shock performance of Pb-free leaded and leadless solder joints is affected by reworking the joints with SnPb eutectic solder. Rework of legacy electronics in military and aerospace systems will necessitate the continued use of SnPb solder for rework for decades. The question this study was focused

on answering is whether SnPb eutectic solder could be used to rework Pb-free solder joints without degrading drop shock performance of the resulting components. If no degradation occurs, only SnPb solder will be required for rework.

This work is part of the larger scale NASA DoD project and utilized the same medium complexity board design, assembly, and rework processes of that larger project.

EXPERIMENTAL-TEST VEHICLE

The test vehicle used for this study, shown in Figure 1, was designed by the Joint Group on Pollution Prevention (JG-PP), the National Aerospace Agency (NASA) and the Department of Defense (DoD) consortia to meet IPC-6012, Class 3 requirements. The 6-layer board with 0.5-ounce copper layers was 368.3mm x 228.6mm x 2.29mm in size. An FR-4 laminate was used as per IPC-4101/26 with a minimum T_g of 170°C. The surface finishes of the boards were Immersion Ag (ImmAg) and ENIG and the pads were non-soldermask defined. The boards were populated with components representative of the parts used for military and aerospace systems. A variety of surface mount technology (SMT) and plated through-hole (PTH) components were daisy chained for electrical monitoring during testing by an event detector. The components monitored are shown in Table 1 below.



Figure 1: Drop Test Vehicle

Table 1: Component Selection

Package	Ball or Finish	Dimensions (mm x mm)	Pitch (mm)	TV-Drop
PBGA225	SAC405 or SnPb	27 x 27	1.5	U02, U04, U04, U06, U18, U21, U43, U44, U55, U56
CSP100	SAC 105	10 x 10	0.8	U19, U32, U33, U35, U36, U37, U42, U50, U60, U63
TQFP-144	Matte Sn	20 x 20	0.5	U01, U03, U07, U20, U31, U34, U41, U48, U57, U58
TSOP-50	Sn	10 x 20	0.8	U12, U25, U29, U39, U61
	SnBi	10 x 20	0.8	U16, U24, U26, U40, U62
PDIP-20	NiPdAu	7.5 x 26	2.5	U8, U23, U49
	Sn	7.5 x 26	2.5	U11, U30, U38, U51, U59
CLCC-20	SAC305	9 x 9	0.8	U09, U10, U13, U14, U17, U22, U45, U46, U52, U53
QFN	Matte Sn	5 x 5	0.6	U15, U27, U28, U47, U54

EXPERIMENTAL – ASSEMBLY AND REWORK

The test vehicles were assembled at the BAE Systems, Irving Texas facility. The Sn3.0Ag0.5Cu (SAC305) solder was chosen for SMT assembly using a conventional reflow profile for SAC305. Then the PTH components were inserted and attached at the TT Apsco Painesville, Ohio facility using Sn0.7Cu0.5Ni ($\leq 0.01\text{Ge}$) (Sn100C) solder. The wave pot temperature was 265°C. Following initial assembly, selected TSOP-50, TQFP-144, QFN-20, and CLCC-20 components were then hand reworked using conventional SnPb (63/37) solder to address the sustainment issue. Both 1x and 2x hand reworks were performed using new components.

Details of the non-BGA rework process were previously published by the authors. [2] BGA rework was performed according to the IPC7711 standard. A hot air rework station with nitrogen was used. Solder paste was applied to the BGA and CSP, not the board. A Pb-free profile with a 245°C peak temperature was used for the mixed Pb-Free/SnPb joints and a conventional 220°C peak temperature profile was used for the pure SnPb joints.

EXPERIMENTAL – DROP TEST

The drop test is used to determine the resistance of board level interconnects to board strain. Boards tested using this method typically fail either as interfacial fractures in the solder joint (most common with ENIG) or as pad cratering in the component substrate and/or board laminate. Outside of laboratory testing, these failure modes commonly occur during manufacturing, electrical testing (e.g. in-circuit test), card handling and field installation and use. The root causes of these types of failures are typically a combination of excessive applied strain due to process issues and/or weak interconnects due to SMT process issues and/or the quality of incoming components and/or boards. This board-level drop test is based on the JEDEC Standard JESD22-B110A

known as Subassembly Mechanical Shock, as well as insight gained by Celestica after performing numerous drop tests on various internal test vehicles over the past 5 years.[3-5]

The drop test process can identify design, process, and raw materials related problems in a much shorter time frame than other development tests. In this project, the drop test was used to determine the operation and strain endurance limits of the solder alloys and interconnects by subjecting the test vehicles to accelerated environments. Unique to this test was the comparison between the interconnect robustness of as-assembled Pb-free leaded components to Pb-free leaded components reworked with SnPb solder. The limits identified in drop testing were used to compare performance differences in the Pb-free test alloy and mixed solder joints vs. the baseline standard SnPb alloy joints. The primary accelerated environments were strain and strain rate.

In this study, a board-level drop shock test was performed on twenty nine assemblies in two sets, one of nine and one of twenty boards, based on the JEDEC test method JESD22-B110A. The only deviation from the JEDEC test was the layout of the test vehicle (see Figure 1). Since the test vehicle was also being used to evaluate many different component types in thermal cycling and vibration tests it did not follow the standard JEDEC layout. However, each board was monitored for shock response and for net electrical resistance for all 63 components using an event detector.

In addition, three of the cards were monitored for surface strain during the drop test. Three cards were dropped with strain monitoring in addition to the shock and resistance monitoring. Four rosette strain gauges were attached to each board at the strain gauge locations shown in Figure 2. Each strain gauge had 3 channels and the principal strain was calculated by using the strain reading from these channels.

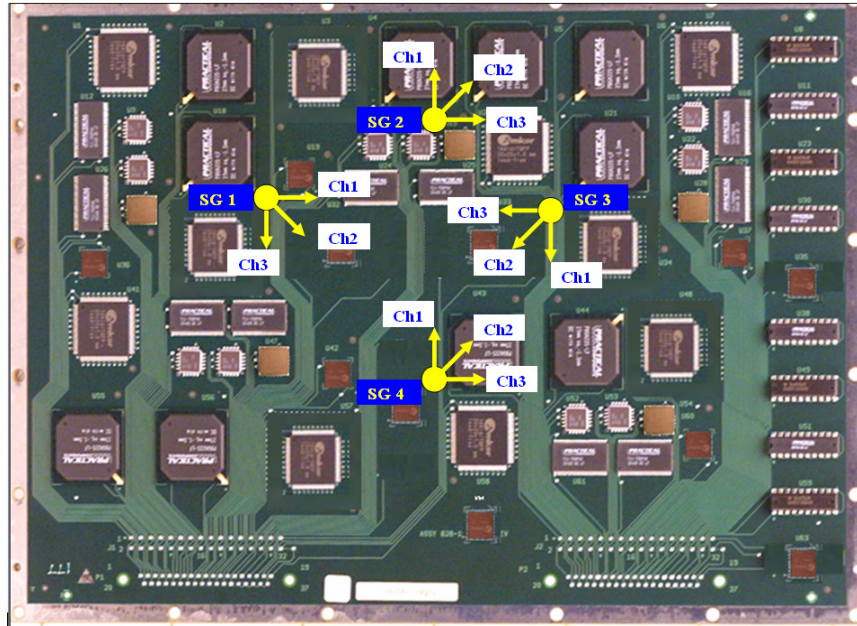


Figure 2: Test Vehicle with Strain Gages, location and orientation illustrated

Three assemblies were fixtured to the drop table at a time with the components facing down and subjected to either 340G or 500G shocks for a total of 20 or 10 drops per board (see Figure 3). The shock response, resistance and strains were recorded in-situ during each drop. A daisy-chain

the Pb-free assemblies. resistance increase greater than 300 ohm from the baseline was considered a failure. Three hundred ohms was chosen based on previous NASA DoD / JG-PP projects. The acceptance criterion was for the reworked cells to have a higher than or an equal number of drops until failure as

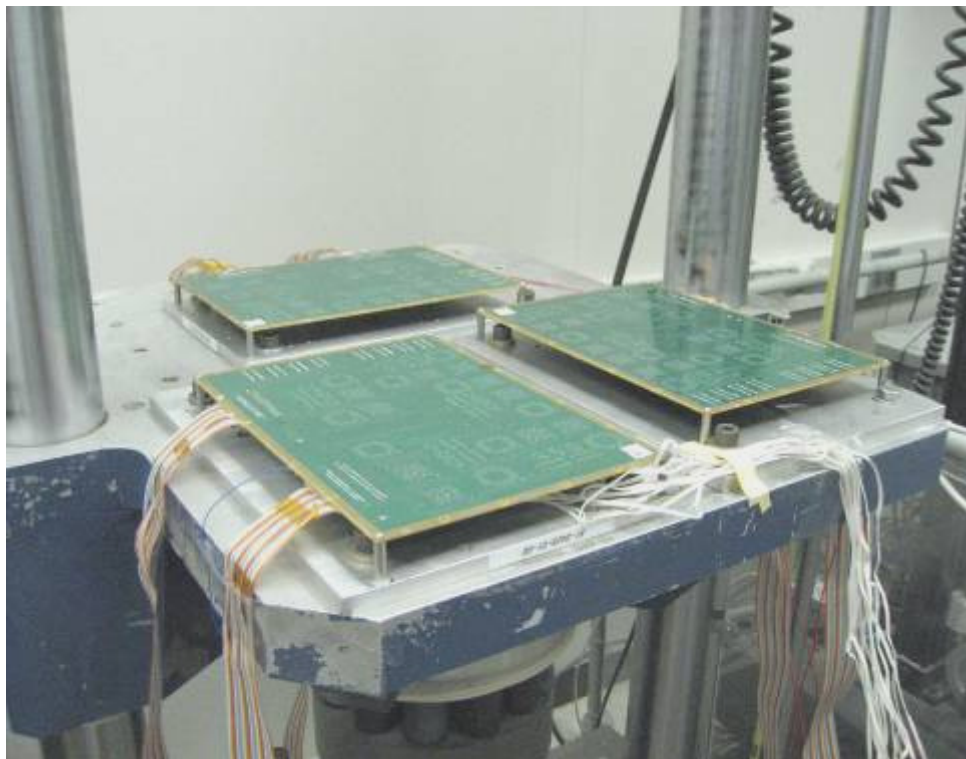


Figure 3: Test Vehicles Mounted on Drop Table

EXPERIMENTAL – FAILURE ANALYSIS

After the drop testing was completed, eight boards from the first set and 11 boards from the second set were selected for destructive failure analysis. Both dye-and-pry and cross sectioning were performed, each of which was designed to determine the location, mode and mechanism of the failure. The samples selected for dye-and-pry were examined using an optical microscope after the parts were pried from the board and the results were further mapped. The cross sectioned samples were examined using optical and scanning electron microscopy (SEM) as well as analyzed by energy dispersive x-ray (EDX). The focus was to compare the quality of the solder joints of components that were reworked once using SnPb solder (therefore consisting of a mixed metallurgy of Pb and Pb-free solder), those that were reworked twice using SnPb solder (consisting of leaded solder), and those which were not reworked at all- therefore Pb-free. The samples selected for destructive failure analysis represented both electrical failures (as determined through resistance monitoring of the components) as well as parts that survived the drop testing with no change to the electrical properties.

MICROSTRUCTURE CHARACTERIZATION

Microstructure characterization of non-BGA components was carried out on three different components TQFP-144, TSOP-50, and QFN-20, each in an as-assembled, 1X rework, and 2X rework condition. The detailed analysis was published by authors in previous paper [2].

Figure 4 shows the microstructure of Pb-free joints before rework. The joints consist of highly branched primary-like Sn dendrites, and $\text{Ag}_3\text{Sn}+\text{Cu}_6\text{Sn}_5+\text{Sn}$ eutectic in interdendritic spaces and between the Sn dendrite arms. Both primary Ag_3Sn platelets and Cu_6Sn_5 were identified by EDX in the TQFP-144 solder joints. Relatively small Ag_3Sn platelets were attached to the pad intermetallic layer. No Ag_3Sn primary platelets were detected in the TSOP-50 solder joints. The primary intermetallic particles in these joints were Cu_6Sn_5 type that contained about 2% Ni and in some cases about 1% Fe. The sources of the Ni and Fe atoms were the Ni barrier layer and the Alloy 42 lead-frame material of the TSOP-50 components. The intermetallic formed between the Cu pads and solder in TQFP-144 and TSOP-50 was rather thin, 1.8 to 2.9 microns, and was of the Cu_6Sn_5 type.

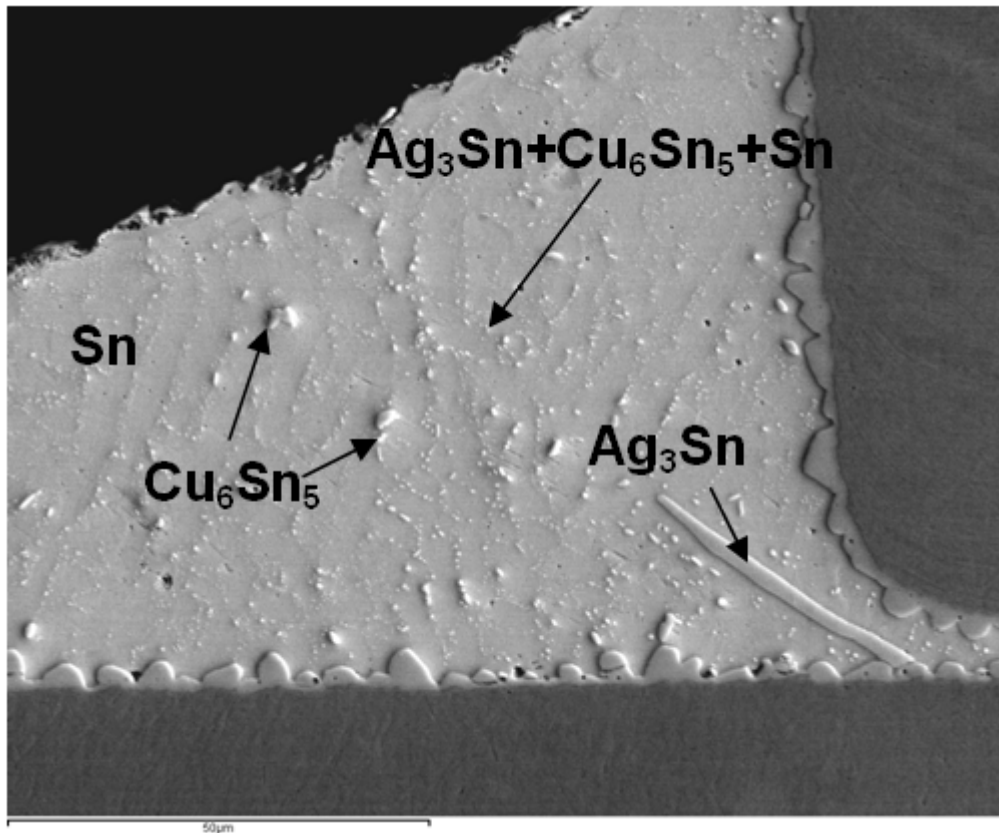


Figure 4: Typical microstructure of SAC305 solder joints before rework, SEM 1000x.

The Pb-free leaded components were reworked with SnPb solder. As expected, the SnPb microstructures of all reworked joints were quite different from that of the assembled Pb-free parts. After 1X rework the joints had a SnPb eutectic structure with some primary intermetallic crystals (Figure). EDX analysis showed that these

intermetallic particles were of the Cu_6Sn_5 type. Some joints also contained some Ni, particularly in the TSOP-50. The number of the primary intermetallic crystals was lower in the QFP-20 reworked joints than in the TQFP-144 and TSOP-50.

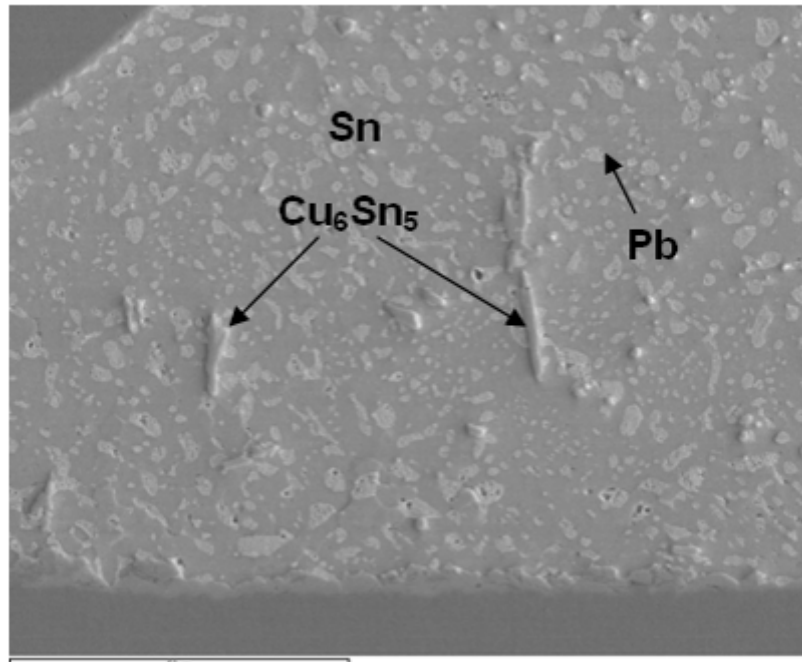


Figure 5: Typical microstructure of 1X reworked solder joints using SnPb solder, SEM, 1000X

A significant portion of primary intermetallic solidifies first, followed by the SnPb eutectic depending on the primary SAC305 alloy composition. The reason for such a significant shift in composition was found in our previous study on ball grid array component rework [5]. During the pad redress step, most of the Pb-free solder left after component removal was consumed by using a Cu solder wick. The rest of the solder was heavily enriched with intermetallic particles. This remaining solder then mixed with the eutectic SnPb alloy used for rework. The excessive intermetallic particles caused a shift in SnPb solder

composition from the near eutectic to off-eutectic. Small intermetallic particles may also be precipitated during cooling from Sn and Pb based solid solutions. These particles were identified as Cu_6Sn_5 . Although an extensive EDX analysis was performed, Ag was not found in reworked solder joints.

After 2X rework, the solder joint microstructure looks like that of a conventional SnPb interconnect - there are no large primary Cu_6Sn_5 crystals present in the solder joint (Figure 6)

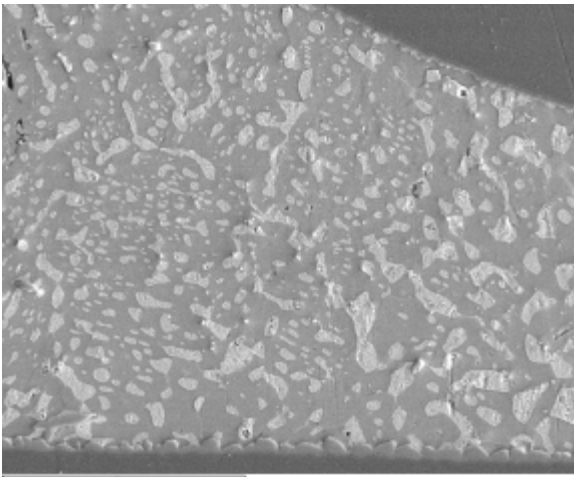


Figure 6: Typical microstructure of 2X reworked solder joints using SnPb solder, SEM, 1000X:

The intermetallic layer formed between the Cu pads and solder in reworked SnPb joints was thinner than in SAC305 as-assembled joints. In the TSOP-50 and QFN-20 it was even thinner after 2X rework. Such a phenomenon was observed by the authors previously and may be explained by dissolution of the intermetallic layer in a fresh solder placed during rework. However, this thickness of intermetallic should not affect the quality or reliability of the solder joints.

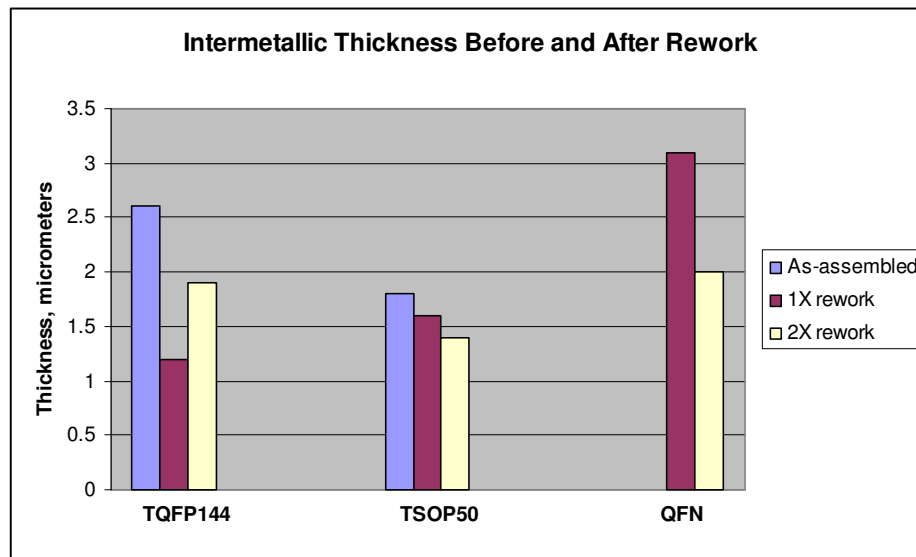


Figure 7: Intermetallic thickness before and after rework.

Combinations of ball materials with solder types used for attachment and rework resulted in the following groups of microstructures : SnPb ball/SnPb solder as assembled; SnPb ball/SnPb solder reworked; Pb-free ball/ Pb-free solder as assembled; SnPb ball/ Pb-free solder as assembled; Pb-free component/ SnPb as assembled; Pb-free component/SnPb solder reworked. The representative microstructures are shown in Figures 8-13.

Both pure SnPb/SnPb and Pb-free / Pb-free solder joints have typical microstructures similar to the non-BGA joints described above (Fig 8, 9). There is no significant difference between as-assembled and rework SnPb/SnPb joints.

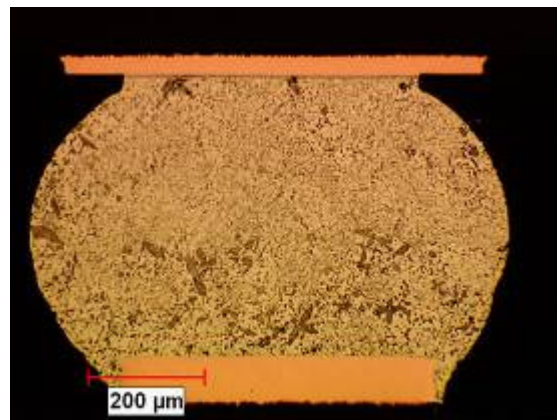


Figure 8. Typical microstructure of pure SnPb/SnPb solder joints.

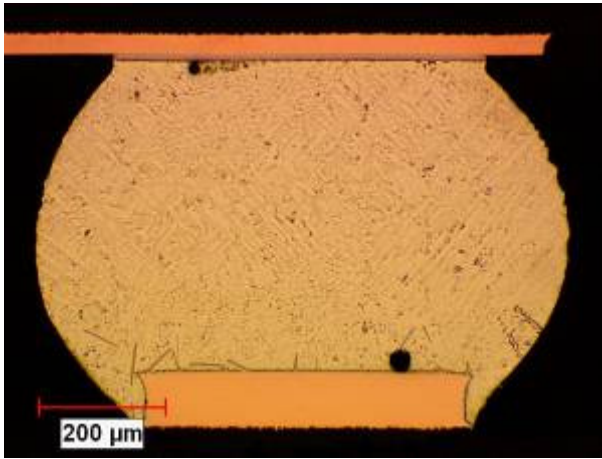


Figure 9. Typical microstructure of pure Pb-free/Pb-free solder joints.

The BGA components with SnPb balls assembled using Pb-free solder demonstrated non-uniform microstructure with at least three clearly distinguished zones (Fig 10). The first zone contains mostly Sn dendrites with Sn+Pb binary eutectic between their branches. The second zone has Sn+Pb eutectic grains with thin Sn+Pb+Ag₃Sn ternary eutectic bands around them. The third zone is an accumulation of the Sn+Pb+Ag₃Sn ternary or even Sn+Pb+Ag₃Sn +Cu₆Sn₅ quaternary eutectic. The details of the second and third zones are shown in a SEM picture (Fig. 11)

Such a complex microstructure is a result of a wide pasty range of an alloy that forms when a SnPb solder ball and SAC305 solder melts together. During reflow cooling, solidification begins at the coldest location with Sn nucleation and growth in a dendritic shape towards the hot board side. The liquid, which is gradually enriching with Pb and Ag and depleting of Sn, finally crystallizes as binary and then ternary eutectic in interdendritic spaces. The last portion of liquid will solidify as a ternary eutectic and/or quaternary at the board side when the temperature of that region reaches about 177°C.

The low melt eutectic accumulation layer that may also contain shrinkage voids at the interface between the Cu or Ni reaction intermetallic layer and bulk solder may be insufficiently strong to withstand stresses experienced during mechanical or thermomechanical testing [7].

Both the assembly reflow profile and rework reflow profile allowed the Pb-free BGA solder ball to be melted and completely mixed with the SnPb solder.

There was no remaining solder ball visible in the microstructure (Fig.12). The phase distribution was more even in this type of joint than in SnPb ball/Pb-free solder, but a low melt eutectic accumulation at the board side in as-

assembled joints and at the component side in rework joints was also detected (Fig.13).

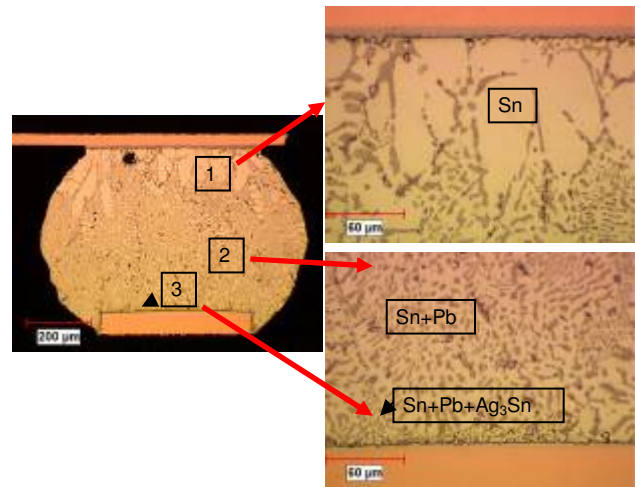


Figure 10. Typical microstructure of mixed SnPb-ball/Pb-free solder joints.

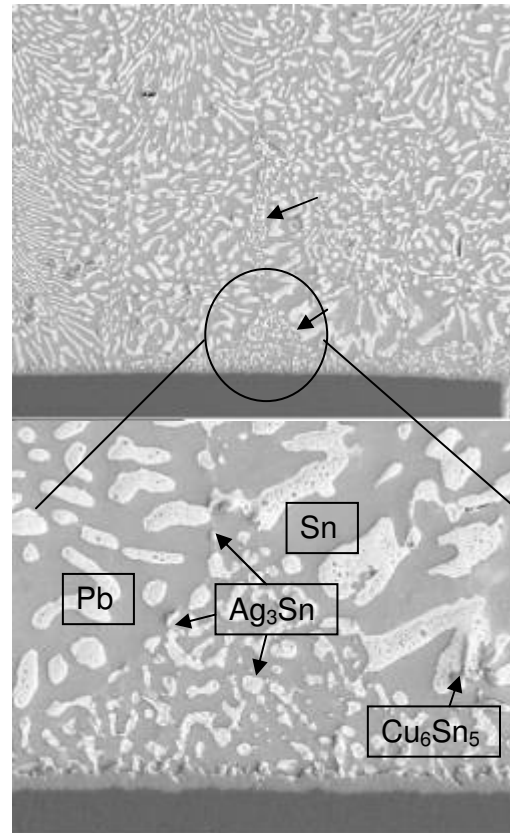


Figure 11. The details of a microstructure of mixed SnPb-ball/Pb-free solder joints showing binary Sn+Pb and ternary Sn+Pb+Ag₃Sn (arrows on top pictures) and phase composition (bottom picture).

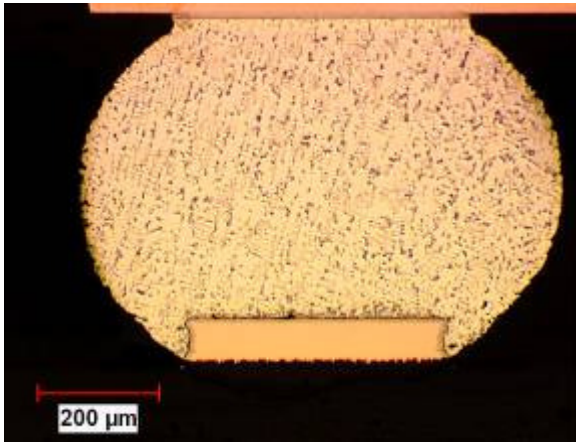


Figure 12. Typical microstructure of mixed Pb-free-ball/SnPb solder joints.

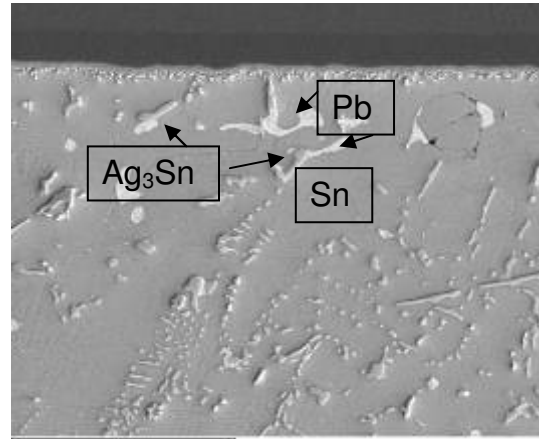


Figure 13. The Sn+Pb+Ag₃Sn eutectic accumulation at the component side of the mixed Pb-free-ball/SnPb solder joints after rework.

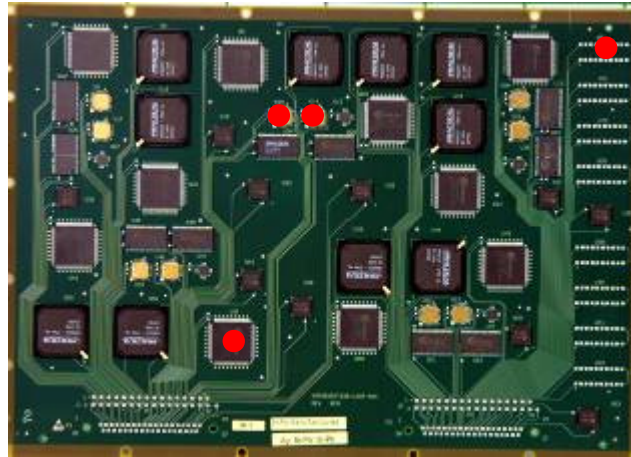


Figure 14: Location of Non-BGA Component Resistance Failures (summary from multiple boards)

RESULTS AND DISCUSSION

Drop Test Results - Leaded components

After each drop, the in-situ resistance data were reviewed and each suspect net was manually checked for a high resistance and the data was recorded. The vast majority of the electrical failures occurred on the PBGAs, none of which were reworked in this first set of cards. Figure 14 shows the physical location of the 4 electrically failing non-BGA components.

Although 477 non-PBGA components were drop tested, only 4 had any increase in net resistance after 20 drops (see Figure 14 above). The 4 non-PBGA components with electrical failure had the following rework histories:

- Board SN 84, CLCC-20, U14 was **not** reworked
- Board SN 85, TQFP 144, U57 was reworked **once**
- Board SN 85, PDIP-20, U8 was reworked **once**
- Board SN 86, QFN-20, U15 was reworked **twice**

Since none of the PBGAs were reworked in this first set of boards and the test resulted in a small number of non-BGA electrical failures, the authors are unable to determine the comparative strength of Pb-free vs. SnPb reworked samples. However, the test does allow the conclusion that the reworked components were in general no worse than the original Pb-free components under these stress conditions and met the strain requirements of the authors.

Drop Test Results - BGAs

Out of the 90 PBGAs drop tested in the 1st set of 9 boards, all but one failed within 20 drops (see Table 2). In addition, all 90 CSP samples passed the electrical monitoring during drop testing.

Table 2: Record of Drops to Electrical Failure for PBGA-225 in the First Set of 9 Boards (Board SN by Component Location)

	82	80	87	86	85	84	83	81	60
U18	12	17	15	10	2	6	9	17	Survive
U56	14	11	13	7	9	8	16	7	14
U55	19	11	19	7	6	3	9	6	15
U2	4	11	14	4	6	4	5	15	17
U4	10	11	6	3	2	4	2	9	6
U43	11	11	6	3	5	6	7	5	8
U21	8	8	10	5	5	3	5	4	5
U44	13	12	10	10	9	7	12	11	16
U5	5	7	5	4	3	2	5	4	4
U6	7	7	5	4	2	2	5	3	3

Figure 15 summarizes average number of drops until electrical failure for the PBGAs in the second set of boards tested. The BGAs were sorted into two groups, areas that experience high board strain during drop testing (near the center of the board) and lower board strain (near the edges of the board). The data is additionally grouped by solder joint composition in Figure 15 below: Red = Mixed (SnPb

solder balls with SAC 305 solder paste). Blue = Not Mixed (pure SnPb joint). Figure 15 clearly shows that BGAs with mixed solder joints failed before pure SnPb BGAs. The difference is most evident in the BGAs in the higher strain areas of the board where mixed BGAs failed 2x sooner on average.

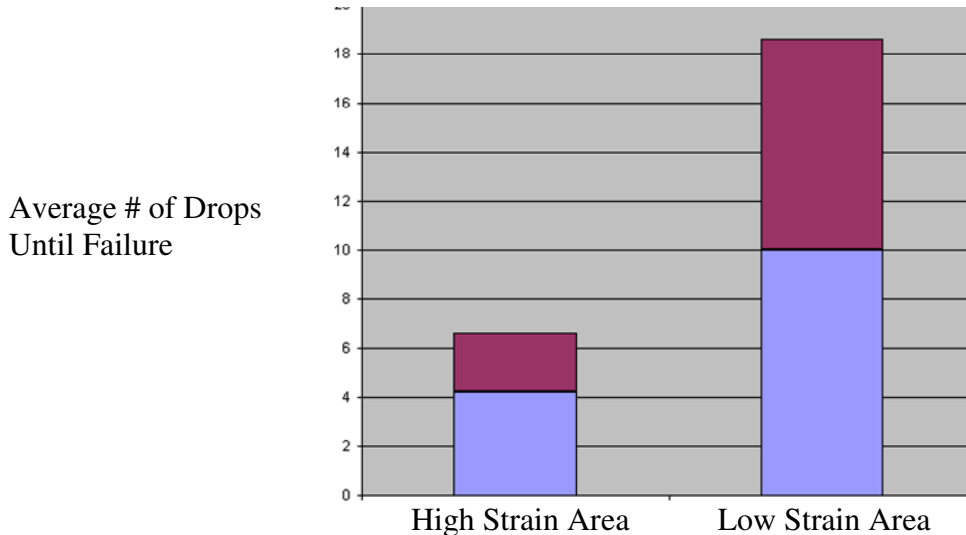


Figure 15: Number of drops until electrical failure for PBGAs. High strain vs. low strain board areas. Red = Mixed (SnPb solder balls with SAC 305 solder paste). Blue = Not Mixed (pure SnPb joint)

Figure 16 below shows that PBGAs in the high strain area that were not mixed survived a higher number of drops before electrical failure occurred. In the mixed state we evaluated two conditions, one in which the solder balls were SnPb and the solder paste was SAC 305 and one in which

the solder balls were SAC 305 and the solder paste was SnPb. Although the sample size was small, the trend shows that mixed joints with SAC 305 in the ball were more robust than those with SnPb balls.

Average # of Drops Until Failure

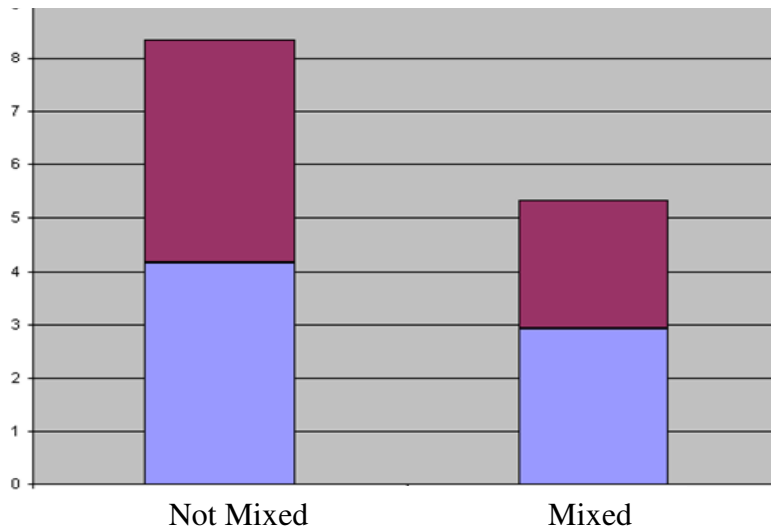


Figure 16: Number of drops until electrical failure for PBGAs in High Strain board area comparing mixed (Yes) to non-mixed(No). Red = Mixed with SnPb balls and SAC 305 paste. Blue = Mixed with SAC 305 balls and SnPb paste.

Figure 17 below shows that for both pure SnPb and pure Pb-free PBGAs in the high strain area, increasing the number of reworks reduced the resilience of the BGAs to drop testing.

Average # of Drops Until Failure

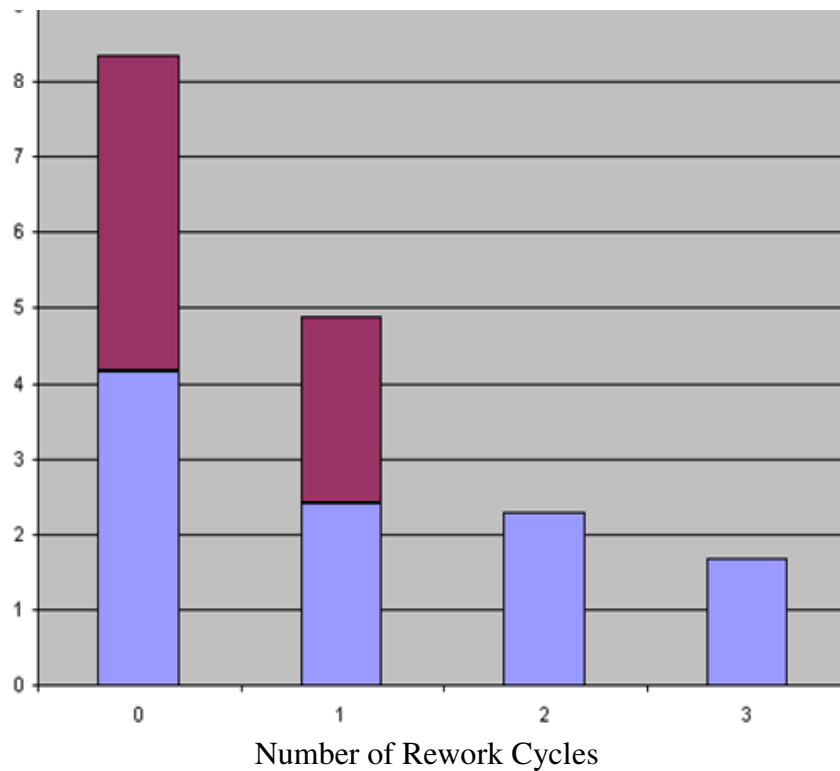


Figure 17: Number of drops until electrical failure for PBGAs in High Strain board area showing the effect of rework. Red = Pure SnPb solder joints. Blue = Pure SAC 305 solder joints.

**Drop Test Physical Failure Analysis
– Non-BGA Parts**

Pad cratering was the predominant failure mechanism in all components, as observed through both dye-and-pry and cross sectioning (Table and Table). In two cases the cratering was significant enough to break the trace and cause an electrical failure. However in most cases the trace

remained intact and therefore no electrical failure was detected. A small number of the analyzed solder joints had signs of solder fracture; however only in one case did this lead to an electrical failure. This indicates that, for the most part, the solder fractures did not penetrate through the entire solder joint.

Table 3: Dye and Pry Mechanical Failures

Board SN	Component					
	CLCC-20	QFN-20		TQFP-144		TSOP-50
60		U15**	U27*	U57*	U58	
81			U27**	U57*		U25*
82					U58*	
83				U57*	U58	U25*
84	U17**	U15**			U58*	
85		U15*		U3		
86			U27*	U57		U25**
87		U15*	U27**		U58	U25*

* represents one rework performed
** represents two reworks performed

Green highlight indicates no failure
Red highlights indicate solder fracture
Orange highlights indicate pad cratering

Table 4: Cross-Sectioning Observations

Board SN	Component						
	CLCC-20	PDIP-20		QFN-20	TQFP-144		TSOP-50
60					U34* *		
81				U15*			
82					U27*	U57	
83		U8* *			U27**		
84	U14						U25**
85						U57*	U58 U25*
86		U8*	U30	<u>U15**</u>			
87				U38			

* represents one rework performed
** represents two reworks performed
Components that are underlined represent electrical failure which occurred during the drop test

Green highlight indicates no failure
Red highlights indicate solder fracture
Orange highlights indicate pad cratering

Pad cratering occurred in all package types (CLCC-20, QFN-20, TQFP-144, TSOP-50) but was less prevalent in the TQFP-144 in which pad cratering was observed on only one out of nine dye-and-pry samples and was not at all found through cross sectioning. This is likely due to the structure

of the part, which has compliant copper leads on all four sides, ensuring efficient stress distribution. However, in one part, the lead was found to fail through the solder in a fatigue failure mode (see Figure 18).

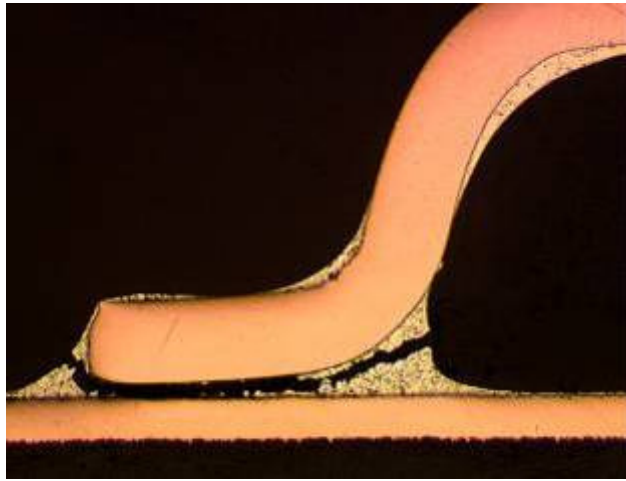


Figure 18: Fatigue failure of TQFP-144 with 1x rework as seen through cross sectioning

Partial solder joint cracks and pad cratering were both observed on the QFN-20 part, at approximately the same frequency. For example, in Figure 19, pin 1 of this QFN-20 package, shows some small evidence of dye penetration through the bulk solder in the top right hand corner of the joint, indicating that a fracture was present prior to prying

the component from the board. The penetration covers less than 25% of the solder surface near the top edge of the joint. Pin 2 shows almost complete dye penetration across the whole pin. The fracture appears to include the intermetallic surface.

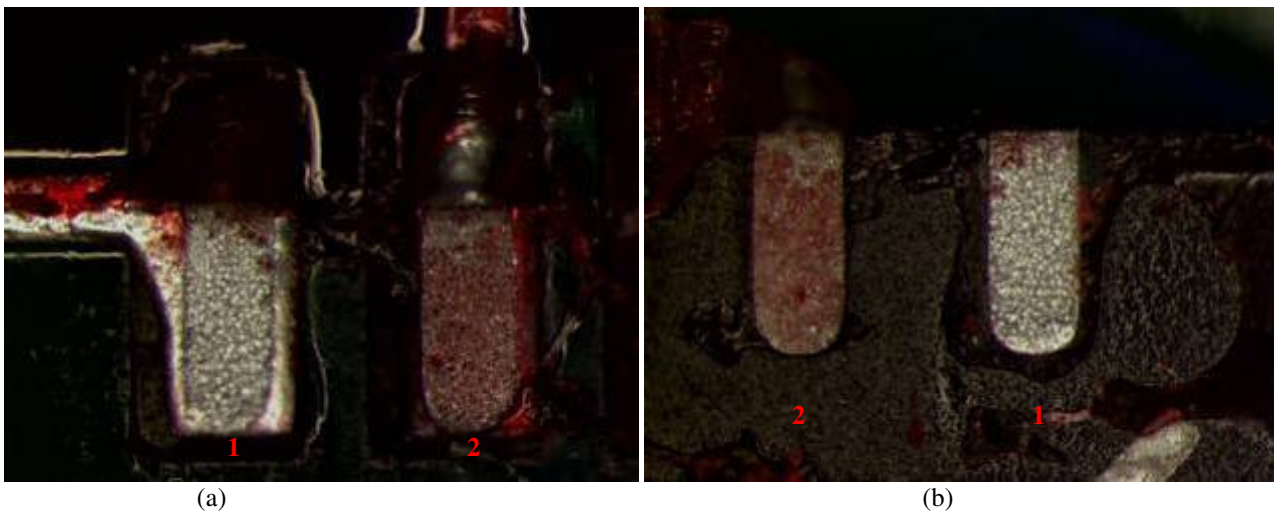


Figure 19: Dye and Pry results of a QFN-20 showing dye penetration through the bulk solder: a- board side; and b- component side

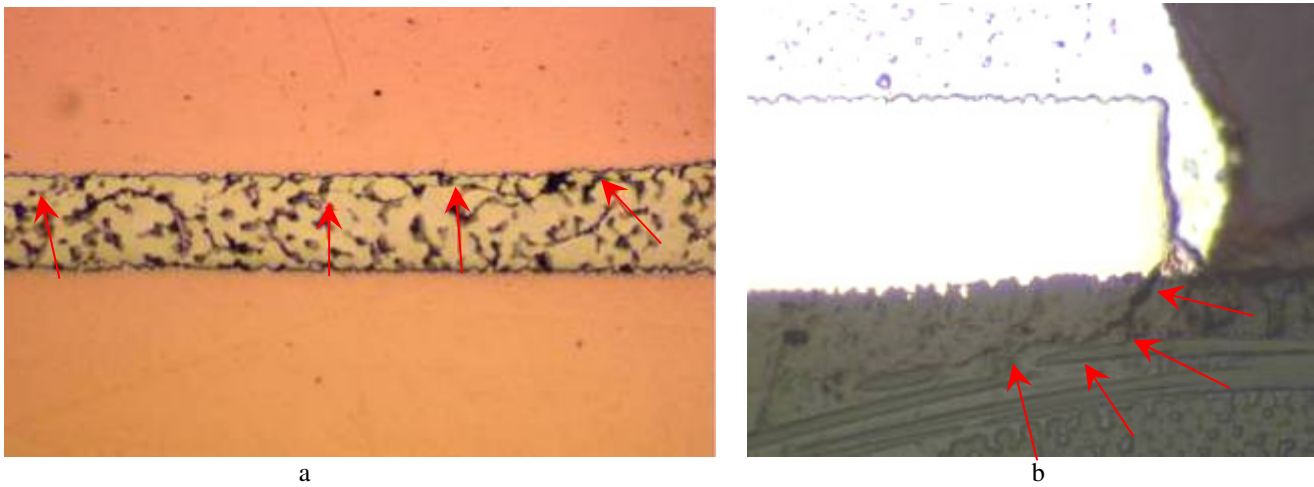


Figure 20: Failures in QFN-20 seen through cross sectioning: a-solder crack at 2x rework; b- pad cratering at 1x rework

Figure 20 shows cross sections which reveal both a fine crack through the bulk solder and pad cratering in a QFN-20 package.

Both the CLCC-20 parts tested and most of the TSOP-50 parts destructively analyzed show some degree of pad

cratering. The cross section in Figure 21(a) illustrates an example of cratering that resulted in a broken trace which can explain the corresponding electrical failure. Figure 21(b) shows the typical pad cratering of a CLCC-20 viewed after dye-and-pry testing.

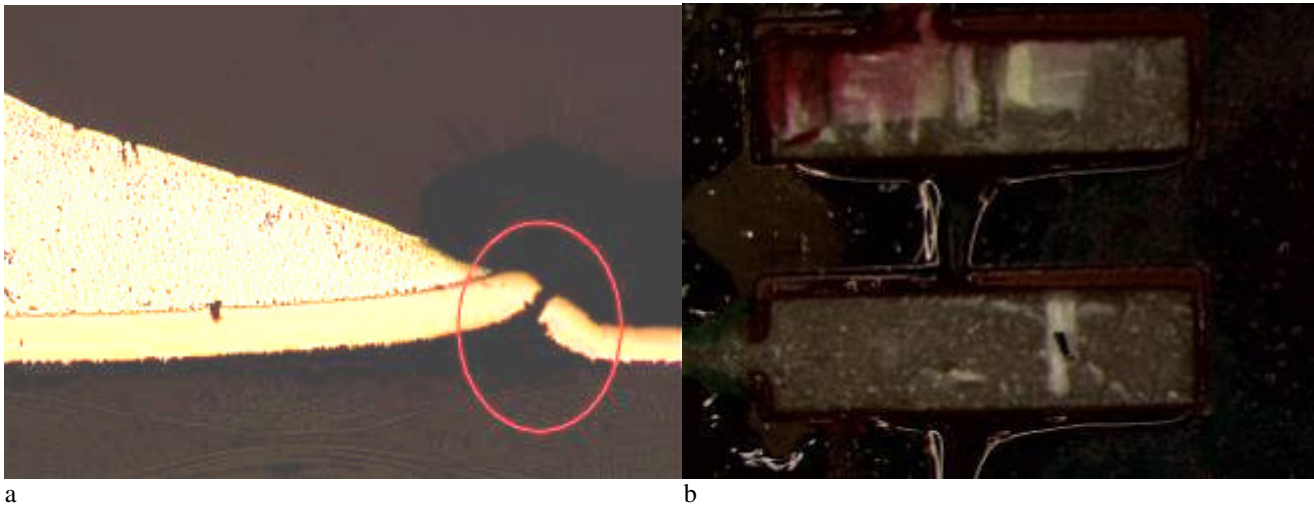


Figure 21: Pad cratering seen on CLCC-20 through: a- cross sectioning; b- dye-and-pry

In this analysis of 23 components, a total of three parts were found to have some mechanical damage in the solder; one of these resulted in an actual electrical failure. In all of these cases, the solder used was SnPb reworked, representing both mixed and SnPb solder. No solder damage were observed in the Pb-free, non-reworked components although the number of samples that were subjected to physical failure analysis would be considered small. All mechanical failures in the Pb-free soldered components were the result of pad cratering. In this study only a small portion of the

components were subjected to failure analysis. More of the components would need to be analyzed in order to increase confidence in the trends observed.

BGA 225 DROP TEST FAILURE ANALYSIS

The predominant mechanism of BGA225 failure mode is also pad cratering. The typical pictures after dye-and-pry and cross-sections of failed joints are shown in Figure 22 and Figure 23, correspondingly.

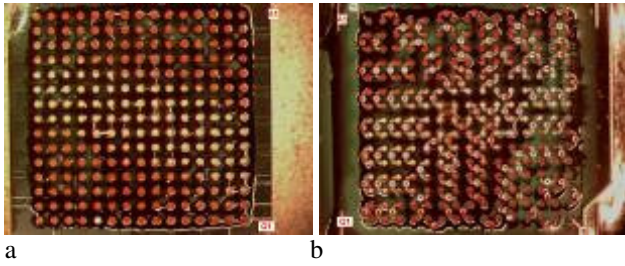


Figure 22. Typical pad cratering seen on BGA225 after dye-and-pry: a – component side; b – board side

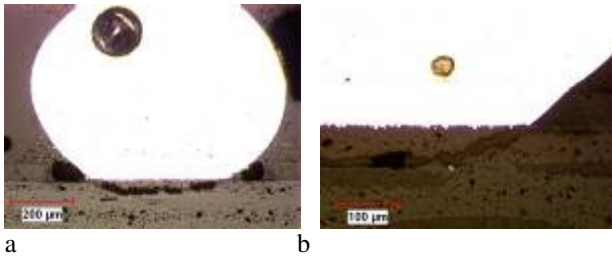


Figure 23. Typical pad cratering seen on BGA225 after cross-section: a – SnPb ball/SnPb solder after rework; b – Pb-free ball/Pb-free solder as-assembled.

An Additional mechanism that caused electrical failure in mixed solder joints was crack propagation through a low melting Sn+Pb+Ag₃Sn ternary and/or Sn+Pb+Ag₃Sn +Cu₆Sn₅ quaternary eutectic accumulation layer at the board or component interface depending on sample history. In as-assembled condition the crack grew between the intermetallic layer and the bulk solder at the board side and after rework the more susceptible location was the interface between the intermetallic layer and the bulk solder at the component side. For the ENIG finished boards the predominant failure modes were brittle intermetallic cracking on both board and component sides (Fig. 24)

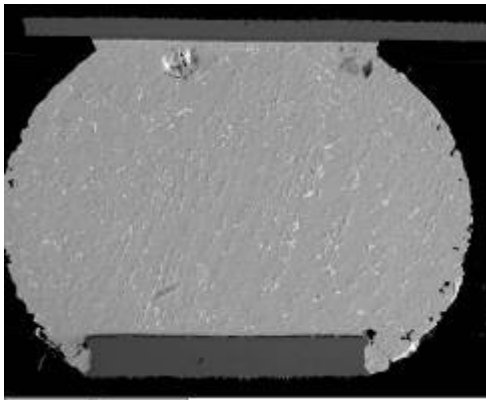


Figure 24. Brittle intermetallic failure seen on BGA225: a- general view;

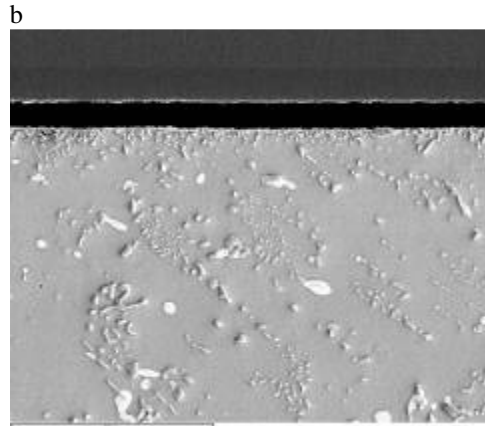
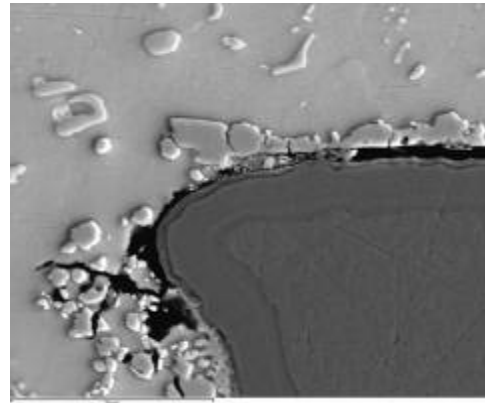


Figure 24. Brittle intermetallic failure seen on BGA225: b – board side; c – component side

CONCLUSIONS

It was found that the drop test reliability greatly depends on the component type. In general, leaded and CSP components are more reliable than large BGAs. The predominant damage mechanism in drop testing is pad cratering. Cracks propagate through the board material between the laminate and glass fiber under the pads. Electrical failure was only observed when the Cu dogbone trace was completely broken. Of the leaded components that were electrically functional after drop testing, approximately one third were found to be mechanically damaged with pad cratering after dye-and-pry inspection. However, only three leaded components electrically failed. There was no correlation found between the number of reworks and the amount of electrical failure since only three leaded components failed in the test. Most importantly, this first sample set showed no difference in drop test performance between SnPb-reworked and non-reworked Pb-free solder joints for non-BGA components. Another important finding is that electrical testing is not sufficient to ascertain non-BGA component interconnect robustness during drop testing. Significant post-test destructive analysis is required to determine the level of mechanical damage. For the PBGAs, although the number of replicate samples evaluated was low due to the large number of variables

drop testing of the PBGA parts showed the following trends: 1) BGAs with mixed SnPb/SAC 305 solder joints failed before pure SnPb BGAs, 2) When joints are mixed, mixed joints with SAC 305 in the ball and SnPb paste were more robust than those mixed with SnPb balls and SAC 305 paste, and 3) for both pure SnPb and pure Pb-free PBGAs, increasing the number of reworks reduced the resilience of the BGAs to drop testing.

FUTURE WORK

Future drop testing should employ a larger number of drops per board if the characteristic failure life of the more compliant non-BGA components is required.

REFERENCES

1. D. Suh, D.W. Kim, P. Liu, H. Kim, J.A. Weninger, C.M. Kumar, A. Prasad, B.W. Grimsley, and H.B. Tejada, "Effects of Ag content on fracture resistance of Sn-Ag-Cu lead-free solders under high-strain rate conditions," *Materials Science and Engineering: A*, vol. 460-461, Jul. 2007, pp. 595-603.
2. P. Snugovsky, J. Bragg, et. al., "Drop Test Performance of a Medium Complexity Lead-Free Board After Assembly and Rework", IPC APEX Expo 2010.
3. J. Bragg, A. Lai and S. Subramaniam, "Strain Induced Assembly and Test Failures", SMTA/CMAP International Conference on Soldering and Reliability, April 2007.
4. J. Bragg, J. Bookbinder, B. Harper and G. Sanders, "A Non-Destructive Visual Failure Analysis Technique for Cracked BGA Interconnects", ECTC 2003 Conference Proceedings, pp. 886-890.
5. J. Bragg, "Pb-Free Failure Analysis Case Studies from an EMS Perspective", SMTAI May 2008.
6. M. Kelly, M. Ferrill, P. Snugovsky, Z. Bagheri, R. Trivedi, G. Dinca and Chris Achong, "Rework Process Window and Microstructural Analysis for Lead-Free Mirrored BGA Design Points", APEX Conf. 2009.
7. "Microstructure, Defect, and Reliability of Mixed Pb-Free/Sn-Pb Assemblies" P. Snugovsky, H. McCormick, S. Bagheri, Z. Bagheri, C. Hamilton, and M. Romansky, *The Journal of Electronic Materials*, Vol. 38, No 2, 2009, pp.292-303.